Advanced Thermo-Hydro-Mechanical modelling features for practical applications in energy geotechnics (Sur la modélisation Thermo-Hydro-Mécanique avancée pour des applications en Géo-énergie)

Bui, T.A.; Casarella, A,; Di Donna, A.; Brinkgreve, Ronald

DOI
10.32075/17ECSMGE-2019-0499

Publication date
2019

Document Version
Accepted author manuscript

Published in
Proceedings of the XVII ECSMGE-2019

Proceedings of the XVII ECSMGE-2019
Geotechnical Engineering foundation of the future
ISBN 978-9935-9436-1-3

doi: 17ecsmge-2019-Y-XXXX

XVII European Conference
ECSMGE 2019
Reykjavik
on Soil Mechanics
and Geotechnical Engineering

Advanced Thermo-Hydro-Mechanical modelling features for practical applications in energy geotechnics

Sur la modélisation Thermo-Hydro-Mécanique avancée pour des applications en Géo-énergie

T.A.Bui (Corresponding / primary author)
Plaxis BV, Delft, Netherlands

A. Casarella; A. Di Donna
Université Grenoble Alpes, Grenoble, France

R.B.J. Brinkgreve
Delft University of Technology / Plaxis bv, Delft, Netherlands

ABSTRACT: Thermal and Thermo-Hydro-Mechanical (THM) analysis is at the core of a broad range of geotechnical engineering applications. In this context, an implicit fully coupled formulation has been implemented in the Finite Element software PLAXIS to perform robustly THM analyses. Advanced constitutive models can be easily defined and implemented with the well-known User-Defined Soil Model (UDSM) module. Recently, another module of User-Defined Flow Model (UDFM) has been developed so that users can implement user-defined fluid and heat transfer models (permeability, thermal conductivity functions etc). These improvements allow to perform advanced research analyses in a practical and user-friendly way. In this paper, the aforementioned formulation and functionalities are briefly summarised. Different examples of benchmark numerical analyses of Engineered Barrier Systems (EBS) in radioactive waste disposals as well as geothermal foundation systems are then presented. The obtained numerical results are verified by comparisons with other simulators and/or experimental data.

RESUME: Les analyses thermiques et thermo-hydro-mécaniques (THM) sont au cœur d'une vaste gamme d'applications de la géo-ingénierie. Dans ce contexte, une formulation implicite couplée a été implémentée dans le logiciel par éléments finis PLAXIS afin de réaliser des analyses THM d'une façon robuste. Les lois de comportement avancées peuvent être facilement implémentées avec le module bien connu «User-Defined Soil Model (UDSM)». Récemment, un autre module de «User-Defined Flow Model (UDFM) » a été développé afin que les utilisateurs puissent implémenter des modèles de transfert de fluide et de chaleur (perméabilité, conductivité thermique etc). Ces améliorations permettent d'effectuer des analyses avancées de manière pratique et conviviale. Dans cet article, ces formulation et fonctionnalités mentionnées sont brièvement résumées. Différents exemples de simulations numériques pour le «Engineered Barier Systems » (EBS) du stockage de déchets radioactifs ainsi que pour les fondations géothermiques sont ensuite présentés. Les résultats numériques obtenus sont vérifiés avec d'autres simulateurs et / ou données expérimentales.

Keywords: Thermo-Hydro-Mechanical coupling; Finite Element Method; Geothermal Energy; Radioactive Waste Disposal

1 INTRODUCTION

Thermal and Thermo-Hydro-Mechanical (THM) analysis is at the core of a broad range of geotechnical engineering applications such as geothermal energy, ground freezing, or deep geologic disposals. Many *modelling features* are required for those advanced applications. In this context, an implicit fully coupled formulation has been implemented in the Finite Element software PLAXIS to perform robustly THM analyses. The formulation is established based on the basis of continuum poromechanics (Coussy, 2004). Advanced constitutive models can be easily defined with the well-known User-Defined Soil Model (UDSM) module. Recently, another module of User-Defined Flow Model (UDFM) has been developed so that users can implement user-defined fluid and heat transfer models (permeability, thermal conductivity functions etc.). These improved *theoretical and implementation features* allow to perform advanced research analyses in a practical and user-friendly way.

In this paper, the aforementioned formulation and functionalities are briefly summarised. Different examples of benchmark numerical analyses of Engineered Barrier Systems (EBS) in radioactive waste disposals as well as geothermal foundation systems are then presented. Different constitutive functions, such as temperature-dependent fluid properties, vapour diffusion, soil-water characteristic curve for unsaturated soil, etc., have been considered to simulate the transient coupled responses of underground structures. The obtained numerical results are verified by comparisons with other simulators and/or experimental data.

2 THEORETICAL FEATURES

PLAXIS generally considers a geomaterial as a 3-phases (solid/liquid/gas) porous medium, but gas pressure is assumed constant, which is widely adopted in geotechnical engineering. In poromechanics, the equations of continuum mechanics are applicable to each phase and to the whole medium. In this section, only the principal equations are briefly revised. For more details, readers may refer to Brinkgreve et al. (2015)

2.1 Mass balance

The mass continuity equation of water writes:

$$n\frac{\partial}{\partial t}(S\rho_w + (1-S)\rho_v) + \\ +(S\rho_w + (1-S)\rho_v)\left[\frac{\partial \varepsilon_v}{\partial t} + \frac{1-n}{\rho_s}\frac{\partial \rho_s}{\partial t}\right] = \\ = -\nabla \cdot \left(\underline{J}_w + \underline{J}_v\right) \qquad (1)$$

Where n (-) is the porosity and S (-) the water saturation. ε_v (-) is the volumetric strain of the soil skeleton and ρ_s, ρ_w and ρ_v (kg/m^3) are the solid, water and gas densities. $\nabla \cdot$ denotes the divergence operator, where ∇ represents the gradient while $\partial/\partial t$ denotes the time derivative. $\underline{J}_w$ and $\underline{J}_v$ (kg/s/m^2) are the mass fluxes of liquid water and vapour, respectively.

2.2 Momentum balance

The linear momentum balance of the whole porous medium is given by:

$$\nabla \cdot \underline{\underline{\sigma}} + \rho \underline{g} = 0 \qquad (2)$$

Where $\underline{\underline{\sigma}}$ (kPa) is the total (Cauchy) stress tensor, $\underline{g}$ (m/s^2) the gravity force vector ρ (kg/m^3) the density of the multiphase medium, defined as:

$$\rho = (1-n)\rho_s + nS\rho_w + n(1-S)\rho_v \qquad (3)$$

2.3 Energy balance

The energy balance equation for the porous medium can be written as follows:

$$\frac{\partial}{\partial t}(nS\rho_w e_w + n(1-S)\rho_v e_v + (1- \\ n)\rho_s e_s) = -\nabla \cdot \left(\underline{J}_{Aw} + \underline{J}_c\right) + Q_T \qquad (4)$$

Where e_w, e_v and e_s (J/kg) are the internal energy in the water, vapour and solid phases, respectively. $\underline{J}_{Aw}$ and $\underline{J}_c$ (W/m^2) are the advective internal energy flux in water and the conductive (diffusive) heat flux in the porous medium, respectively. Q_T (W/m^3) is the heat source term, i.e. heat generation rate per unit volume.

2.4 Some basic constitutive laws

The stress and flux terms in the above balance equations can be specified by the following basic constitutive laws.

2.4.1 Effective stress concept

For partially saturated soils the Bishop's effective stress (Bishop & Blight, 1963) is used:

$$\underline{\underline{\sigma'}} = \underline{\underline{\sigma}} - S_e p_w \underline{\underline{I}} \qquad (5)$$

Where $\underline{\underline{\sigma'}}$ (kPa) is the effective stress tensor, p_w (kPa) the pore water pressure, $\underline{\underline{I}}$ (-) the second order identity tensor and $S_e = \frac{S - S_r}{S_s - S_r}$ (-) is the effective saturation with S_s and S_r are the saturated and residual saturation degrees. This effective stress parameter varies from 0 (fully dry) to 1 (fully saturated) conditions.

2.4.2 Non-isothermal unsaturated flow

Due to the full triply-coupled thermo-hydro-mechanical process, the description of groundwater flow occurring in an unsaturated medium needs to take into account the occurrance of vapour flow in the pores and the thermal effects on mass water and mass vapour fluxes. In light of the above, an extended Richard's model is applied to describe non isothermal unsaturated flow. The mass flux of water is defined as Rutqvist et al. (2001):

$$\underline{J}_w = \rho_w(T)\underline{q} = \\ = \rho_w(T)\left(\frac{k_{rel}}{\mu(T)}\underline{\underline{\kappa}}^{int}\left(\nabla p_w + \rho_w(T)\underline{g}\right)\right) \qquad (6)$$

Where $\mathrm{k_{rel}}$ (-) is the relative permeability of the medium, μ (kPa·s) is the dynamic viscosity and depends on temperature T (K), $\underline{\underline{\kappa}}^{\mathrm{int}}$ (m^2) is a tensor containing the intrinsic permeabilities of the porous medium in the three principal directions.

In parallel, the mass flux of vapour in non-isothermal processes is defined as:

$$\underline{J}_v = -D_v \nabla \rho_v = D_{pv} \nabla p_w - D_{Tv} \nabla T \qquad (7)$$

Where T is the local equilibrium temperature od the porous mediu:m, D_v is the vapour diffusion coefficient and D_{pv} and D_{Tv} are hydraulic and thermal diffusion coefficients.

2.4.3 Heat transfer law

The conductive heat flow (Eq. (4)) is assumed to be governed by Fourier's law:

$$\underline{J}_c = -\lambda \nabla T \qquad (8)$$

Where λ is the thermal conductivity of the multiphase medium calculated by:

$$\lambda = (1-n)\lambda_S + nS\lambda_w + n(1-S)\lambda_v \qquad (9)$$

$\lambda_S, \lambda_w, \lambda_v$ are the solid, water and vapour conductivities.

On the other hand, the advective heat flux in (4), which represents the heat transported by water flow, is given by :

$$\underline{J}_{Aw} = C_w T \underline{J}_w \qquad (10)$$

3 IMPLEMENTATION FEATURES

3.1 Discretisation scheme

The equations were implemented so that both degrees of freedom (displacements, temperature and water pore pressure) are solved within the same time step. This fully coupled scheme is

physically realistic as it does not need any further "decoupling" assumptions within each step.

Triangular elements, either 6-noded (quadratic) or 15-noded (fourth order) can be used. Those elements allow to model irregular geometries with a rich interpolation.

An implicit scheme is used for time discretisation (Brinkgreve et al., 2015) for parabolic systems. The time marching scheme is automatic where time step is adjusted according to convergence rate and accuracy. This allows for a much more relaxed and robust step size compared to explicit schemes where stability condition often restricts a very small time step.

3.2 User-defined models

Apart from many built-in geomaterial models provided in the software library, users may also define their own material models with the well-known User-Defined Soil Model (UDSM) module. Recently, another module of User-Defined Flow Model (UDFM) has been developed so that users can implement user-defined fluid and heat transfer models.

Both functionalities have the same concept: they can be easily implemented by in the form of a dynamic link library (dll) which can be loaded by PLAXIS. Those dlls can exchange information (strain-stress in the case of UDSM, and flow functions such as permeability or thermal conductivity in the case of UDFM) with the calculation kernel to provide desired responses. This enhances enormously the flexibility for advanced research and engineering projects.

4 CASE STUDY 1: RADIOACTIVE WASTE DISPOSAL

This study is part of the EBS project initiated by the Swedish Nuclear Fuel and Waste Management Company (SKB), in order to develop effective tools for the advanced multi-physics analysis of buffer and backfill behavior. One of the tasks consists in simulating with different simulators, a benchmark model to verify and enhance THM modelling capability (Schäfers et al., 2018). In the following, one part of the benchmark, which aims at modelling the TH couplings in unsaturated buffer is described.

4.1 Model definition

The benchmark model is a 2D axisymetric representation of a single KBS-3V deposition hole. During the first phase, an initial temperature of 25°C is set up and a hydraulic calculation is performed to simulate the steady-state pore pressure distribution in a crystalline rock mass after hole opening process. During the second phase, an initially unsaturated backfill is installed together with a waste canister. The latter is not explicitely represented but modelled by appropriate boundary conditions. Concretely, a time-dependent thermal flux corresponding to the heat decay of the canister (Figure 1) is applied. Detailed geometry, boundary conditions and generated mesh are described in Figure 2.

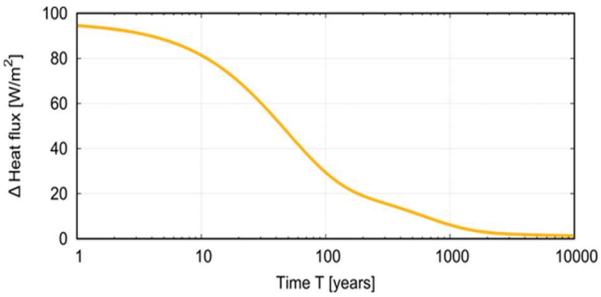

Figure 1. Canister power decay

The benchmark requires modelling of complex phenomena using the above advanced features:

- Temperature-dependent fluid properties with vapour diffusion (incorporated in the general framework in Section 2)
- Specific transfer laws for bentonite using the UDFM feature (section 3)

More precisely, thermal conductivity and vapour diffusivity coefficient of bentonite are functions of saturation degree S:

$$D_v = 2.16\,10^{-5}(1-S)n\left(\frac{T}{273.15}\right)^{1.8} \qquad (11)$$

$$\lambda = 0.7 + 0.6S \quad (12)$$

while water retention and relative permeability are modelled by the following empirical laws:

$$S = \left[1 + \left(\frac{-p_w}{P_{B0}}\right)^{\frac{1}{1-m_B}}\right]^{-m_{B0}} \left[1 - \frac{\phi}{P_{B1}}\right]^{m_{B1}} \quad (13)$$

$$k_{rel} = S^3 \quad (14)$$

With $m_{B0}, m_{B1}, P_{B0}, P_{B1}$ are model parameters. For rock material, constant vapour diffusivity and thermal conductivity and standard Van Genuchten (V-G) models are used (see (Brinkgreve et al., 2015)).

Only the main general parameters are summarised in Table 1. Other details about the benchmark modelling and specific parameters can be found in Schäfers et al. (2018).

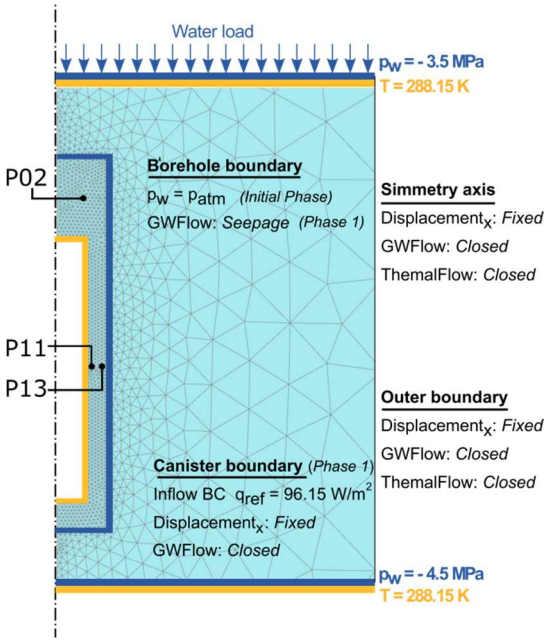

Figure 2 Model mesh and boundary conditions

Table 1. Soil parameters surrounding the pile

Parameter	Symbol	Rock	Bentonite	Unit
General				
Dry soil unit weight	γ_{unsat}	26.41	15.33	kN/m^3
Initial void ratio	e_{init}	0.003	0.779	-
Hydraulic				
Intrinsic isotropic Permeability	k	$1 \cdot 10^{-10}$	$6.4 \cdot 10^{-14}$	m/s
Thermal				
Specific heat capacity	c_s	770	800	J/kg/K
Thermal conductivity	λ_s	2.4	Eq.12	W/m/K
Solid density	ρ_s	2700	2780	kg/m^3
Thermal expansion	α_s	$7.2 \cdot 10^{-6}$	$3.4 \cdot 10^{-6}$	1/K

4.2 Numerical results and validation

In the following, the results at different observation points P02, P11 and P13 (Figure 2) are plotted. For each plot, Code-Bright and OGS results (drawn from Schäfers et al. (2018)) are superimposed on PLAXIS blue curve in order to perform code comparison.

In Figure 3a, temperature evolution over time is plotted. At both locations the temperature rises with the heat supply but then at large time decreases due to the decay of the heat source. Owing to the proximity from P11 to the hot boundary (only 5 cm), temperature in P11 rapidly increases. Greater the distance from the canister, lower the slope of the curve and thus lower the maximum temperature value ever reached in the points (P02 and P13). Both simulators provide very similar results with the maximum recorded difference around 1%.

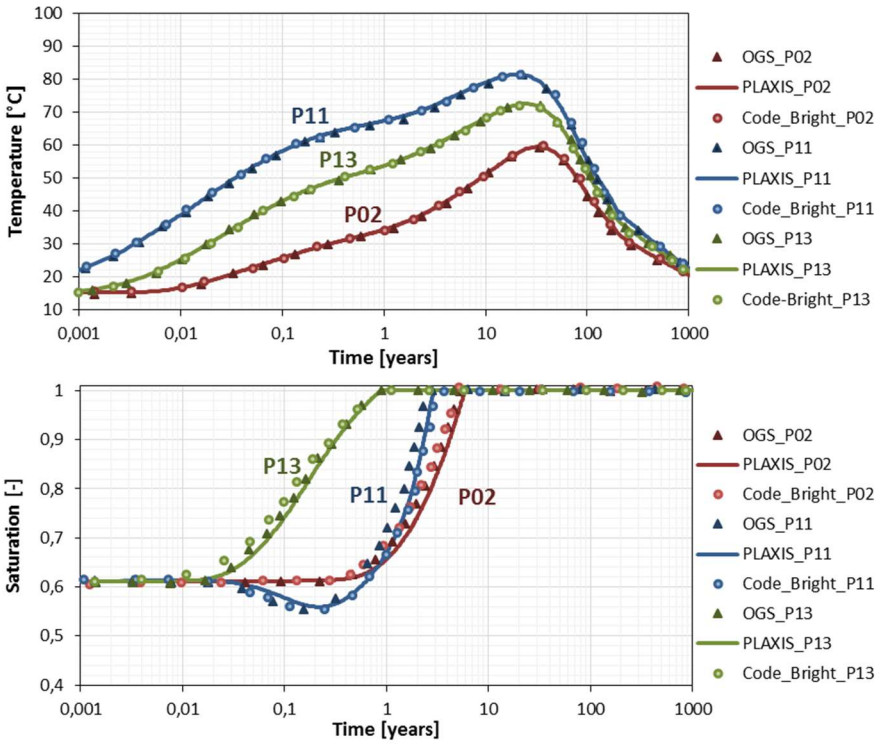

Figure 3 Numerical results and comparisons between different codes

The same good match between the codes is observed for saturation (Figure 3b). Starting from an initial saturation value of 61%, the saturation evolves with 2 competing phenomena: vapour diffusion (thermal drying) and water penetration from the rock mass (hydraulic wetting). As heat supply from the canister is decreasing with time, vapour diffusion only has a short time effect and it is only visible at P11 (which is very close to the heat boundary) where the saturation is decreased after a couple of months. At large times, all the points are fully resaturated with the wetting process. Similar evolution can be seen for the pore water pressure (Figure 3b). A good agreement between the three simulators is observed, with a difference of less than 6%.

5 CASE STUDY 2: GEOTHERMAL FOUNDATION

Recently there has been an increase in use of heat pile for exploiting geothermal energy. Pile heat exchangers are deep foundations having the double role of providing structural stability and extracting renewable and clean source of energy for heating and cooling buildings. Thus heat pile design would require THM analysis to ensure its two-fold role. In this chapter, the in-situ experiment on the behaviour of a single heat pile (Laloui et al., 2003) will be simulated using the above THM framework.

5.1 Model definition

The numerical model consists of an axisymetric representation of the model with a concrete pile (length of 26m and diameter of 1m) embedded in a stratified ground. The ground is extended far enough to ensure an impertubation at far-field. To simplify, a perfect contact between the pile shaft and soil is considered, although more realistic models with interface elements can also be used. The corresponding mesh is shown in Figure 4.

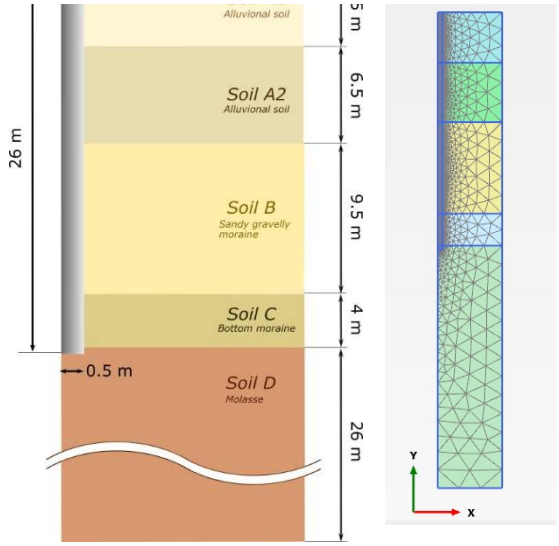

Figure 4 Model geometry and mesh

Plastic pipes and circulating fluid are not modelled and only a thermal boundary condition is applied to the pile-soil interface. The initial, as well as the far-field (unaffected) temperatures are fixed at 15°C. Radial displacements and flow are fixed at the symmetry axis, while the head of the pile is not restrained because no mechanical loads are considered in this test. According to Laloui et al. (2003), a constant temperature of 15° is applied to the top surface to simulate the atmosphere temperature and a heating-cooling cycle (Figure 5) is applied to the pile shaft boundary to simulate heat exchange by the pile. The propeties of the soil layers are taken from Laloui et al. (2003) and Di Donna et al. (2015) and listed in Table 1.

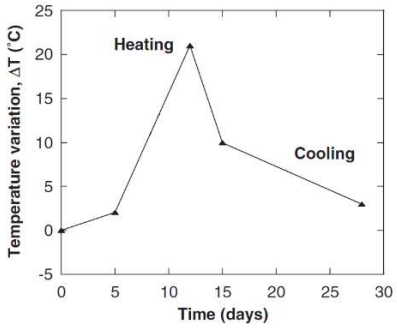

Figure 5. Heating-cooling cycle applied on pile shaft.

5.2 Numerical results and validations

Figure 6 shows the temporal vertical pile displacement. A good agreement is observed. between the obtained numerical results and the experimental ones mesured by different techniques reported in Laloui et al. (2003). As expected, the imposed thermal field generates strains and displacement in the pile due to thermal expansion.

Table 2. Soil parameters surrounding the pile **MC=Mohr-Couloimb; LE=Linear Elastic*

Parameter	Symbol	Concrete	Soil A1	Soil A2	Soil B	Soil C	Soil D	Unit
General								
Material model*	*Model*	LE	MC	MC	MC	MC	MC	-
Wet unit weight	γ_{sat}	25.0	26.0	25.35	21.27	22.18	25.5	kN/m^3
Initial void ratio	e_{init}	-	0.111	0.111	0.538	0.429	-	-
Mechanical								
Stiffness	E'	$2.92\cdot10^7$	$2.6\cdot10^5$	$2.6\cdot10^5$	$8.4\cdot10^4$	$9.0\cdot10^4$	$2.6\cdot10^6$	kN/m^2
Poisson's ratio	ν'	0.1769	0.1461	0.1461	0.4	0.4	0.1517	-
Cohesion	c'	-	5	3	6	20	-	kPa
Friction angle	φ	-	30	27	23	27	-	°
Dilatancy angle	ψ	-	7.5	7.5	7.5	7.5	-	°
Hydraulic								
Permeability	k	0	$2.0\cdot10^{-6}$	$7.0\cdot10^{-7}$	$1.0\cdot10^{-5}$	$2.0\cdot10^{-10}$	0	m/s
Thermal								

Specific heat capacity	c_s	800	863	863	890	890	784	J/kg/K
Thermal conductivity	λ_s	2.1	1.8	1.8	4.45	4.17	1.1	W/m/K
Solid density	ρ_s	2500	2780	2780	2735	2740	2550	kg/m^3
Thermal expansion	α_s	$1.0 \cdot 10^{-5}$	$1.0 \cdot 10^{-5}$	$1.0 \cdot 10^{-5}$	$1.0 \cdot 10^{-4}$	$1.0 \cdot 10^{-4}$	$1.0 \cdot 10^{-6}$	1/K

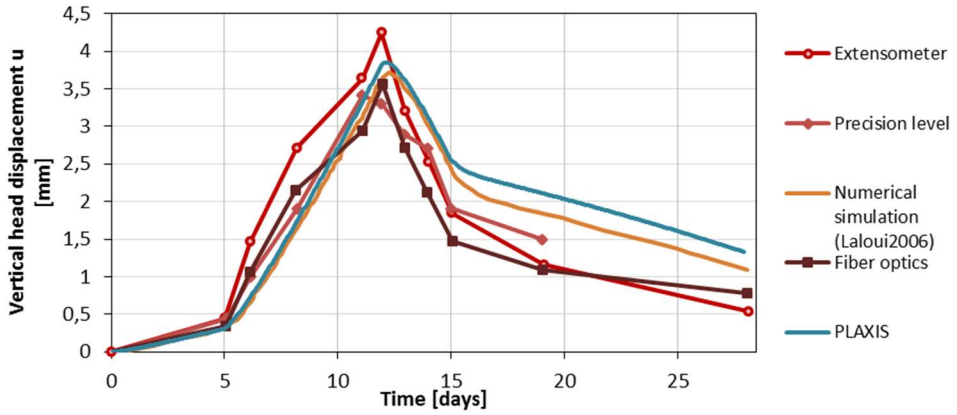

Figure 6. Verical head displacement during the heating-cooling cycle.

6 CONCLUSIONS

Advanced modelling features, including theoretical and implementation aspects, have been developed in the finite element software PLAXIS. The features allow to perform complex THM modelling in a rigorous but robust and user-friendly way. This has been illustrated in two advanced numerical examples for the radioactive waste disposal and geothermal foundation.

7 REFERENCES

Brinkgreve, R.B.J., Engin, E., Swolfs, W.M. (2015). PLAXIS 2D 2015, *Thermal and Thermo-Hydro-Mechanical analysis*. Delft: Plaxis bv

Coussy, O. 2004. *Poromechanics.* Chichester: John Wiley & Sons LTd

Bishop, W., Blight, E. 1963. Some aspects of effective stress in saturated and partly saturated soils. *Géotechnique* **13**, 177-197.

Rutqvist, J., Börgesson, L. Chijimatsu, M., Kobayashi, A., Jing, L., Nguyen, S., Noorishad, J., Tsang, C. 2011. Thermohydromechanics of partially saturated geological media: Governing equations and formulation of four finite element models **38**, 105-127.

Laloui, L., Moreni, M., Vulliet, L., 2003. Comportement d'un pieu bi-fonction, fondation et échangeur de chaleur, *Candian Geotechnical Journal* **40**, 388–402.

Di Donna, A., Rotta Loria, A.F, Laloui, L. 2015. Numerical study of the response of a group of energy piles under different combinations of thermo-mechanical loads. *Computers and Geotechnics* **72**, 126–142.

Schäfers, A., Gens, A., Rodriguez-Dono, A., Baxter, S., Tsitsopoulos, V., Holton, D., Malmberg, D., Sawada, M., Yafei, Q., Ferrari, A., Laloui, L., Sjöland, A. 2018. Increasing process understanding and confidence in simulations - sensitivity studies and code comparison of coupled THM simulations within the Task Force on Engineered Barrier Systems. *Environmental Geotechnics* (under review)